AIP Applied Physics Letters

Topological charge transfer in frequency doubling of fractional orbital angular momentum state

R. Ni, Y. F. Niu, L. Du, X. P. Hu, Y. Zhang, and S. N. Zhu

Citation: Applied Physics Letters **109**, 151103 (2016); doi: 10.1063/1.4964712
View online: http://dx.doi.org/10.1063/1.4964712
View Table of Contents: http://scitation.aip.org/content/aip/journal/apl/109/15?ver=pdfcov
Published by the AIP Publishing

APPLIED PHYSICS LETTERS **109**, 151103 (2016)

Topological charge transfer in frequency doubling of fractional orbital angular momentum state

R. Ni,[1] Y. F. Niu,[1] L. Du,[1] X. P. Hu,[1,a)] Y. Zhang,[2] and S. N. Zhu[1]
[1]*National Laboratory of Solid State Microstructures and School of Physics, Nanjing University, Nanjing 210093, China*
[2]*College of Engineering and Applied Sciences, Nanjing University, Nanjing 210093, China*

(Received 21 June 2016; accepted 29 September 2016; published online 10 October 2016)

Nonlinear frequency conversion is promising for manipulating photons with orbital angular momentum (OAM). In this letter, we investigate the second harmonic generation (SHG) of light beams carrying fractional OAM. By measuring the OAM components of the generated second harmonic (SH) waves, we find that the integer components of the fundamental beam will interact with each other during the nonlinear optical process; thus, we figure out the law for topological charge transfer in frequency doubling of the fractional OAM state. Theoretical predictions by solving the nonlinear coupled wave equations are consistent with the experimental results. *Published by AIP Publishing.* [http://dx.doi.org/10.1063/1.4964712]

Light beams carrying orbital angular momentum (OAM)[1] have attracted increasing attention in the past years due to the wide applications in optical tweezers,[2] optical trapping,[3] imaging,[4] and information processing.[5,6] To imprint OAM onto light beams, several methods have been exploited, including spiral phase plates,[7] Q-plates,[8,9] diffraction gratings,[10] and manipulation of modes in laser cavities[11] and on meta-surfaces.[12] Besides, nonlinear frequency conversion has been proved to be an alternative for generating OAM states with higher order and shorter wavelengths.[13–19] In general, the topological charge of OAM state can be either integer or fraction. In most of the work on nonlinear frequency conversions with an integer OAM input, the topological charges were reported to be conserved. While work on nonlinear frequency conversion of fractional OAM state are rare. Using light beam carrying fractional OAM state as the pump, very high-dimensional spatial entanglement of twin photons was experimentally demonstrated through spontaneous parametric down-conversion, which will have applications in high-capacity quantum communications.[20] As for frequency up-conversions, in Ref. 21, second harmonic generation (SHG) of the fractional OAM state was investigated, confirming the OAM conservation selection rule by analyzing the recorded second harmonic (SH) field. The fractional OAM state is a superposition of infinite integer OAM modes,[22] so, in principle, the nonlinear frequency conversion of the fractional OAM state should be more complicated compared with that of a pure integer OAM state. In this paper, we investigate SHG of the fractional OAM state using the coupled wave equations, taking into account the interactions between the integer OAM components. Experimental results on measuring the topological charge distribution of both the fundamental wave (FW) and SH waves were in good agreement with the theoretical predictions.

Assuming the field of the integer OAM component of the FW to have the form $E_i^{(n)} = B_i^{(n)}(z)u_i^{(n)}(\rho, z)e^{in\varphi}e^{ik_i z}$, where $B_i^{(n)}$ is the field amplitude, $u_i^{(n)}$ is the transverse field distribution, n is the topological order, and k_i is the wave vector. Substitute $E_i^{(n)}$ into the well-known coupled wave equations in the textbooks,[23] a set of coupled wave equations can be written to describe the SHG of the fractional OAM state (see the supplementary material for detailed derivations)

$$\frac{dB_3^{(l)}}{dz} = \sum_{n,m=-\infty}^{+\infty} \frac{i\omega_3}{n_3 c} d_{\mathrm{eff}} B_1^{(n)} B_2^{(m)} \gamma^{(1,2)} e^{i\Delta kz} e^{i(n+m-l)\varphi}, \quad (1)$$

$$\frac{dB_i^{(n)}}{dz} = \sum_{l,m=-\infty}^{+\infty} \frac{i\omega_i}{n_i c} d_{\mathrm{eff}} B_3^{(l)} B_j^{*(m)} \gamma^{(j,3)} e^{-i\Delta kz} e^{-i(n+m-l)\varphi}. \quad (2)$$

In the equations, $l = \ldots -2, -1, 0, 1, 2\ldots$ is the topological charge of the integer OAM component of the SH wave, $m, n = \ldots -2, -1, 0, 1, 2\ldots$ represent that of the FW. To ensure OAM conservations, $l = m + n$ is required. The index $i, j = 1, 2$ $(i \neq j)$ represents the integer components of the FW, while 3 represents that of the SH. ω_i is the angular frequency, n_i is the refractive index, and c is the speed of light, respectively. d_{eff} is the nonlinear coefficient of the second-order nonlinear optical process. It is dispersive and is dependent on the polarization of the electrical field of the interacting waves. $\Delta k = k_{SH} - 2k_{FW}$ is the wave-vector mismatch between the SH and the FW, and this wave-vector mismatch can be compensated for if phase-matching techniques are exploited.[24] γ is the spatial overlapping integral between the interacting waves, and the definition is clarified in the supplementary material.

The experimental setup is mainly composed of three parts, as shown in Figure 1. The first part is to prepare the FW carrying fractional OAM, including a nanosecond laser operating at 1064 nm, a beam expander, a phase-only spatial light modulator (SLM), and a Fourier-transform system. The fractional helical wave-front is imprinted on the FW with the SLM which can display a computer calculated holograms.[25] An aperture was placed in the Fourier plane after the SLM to select the desired diffraction order. In the second part, frequency doubling of the incident wave is performed at room

a)Author to whom correspondence should be addressed. Electronic mail: xphu@nju.edu.cn

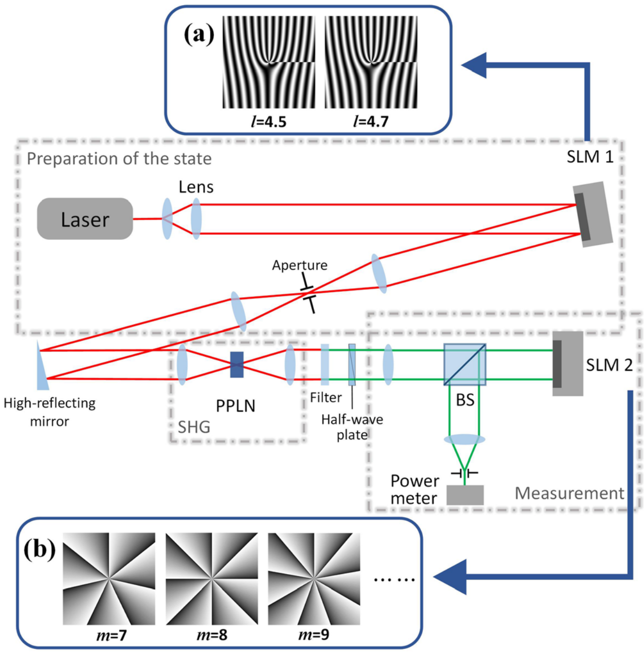

FIG. 1. Schematic experimental setup for studying SHG of light beams carrying fractional OAM. The setup is comprised of three parts: preparation of the OAM states, SHG of the fractional OAM states, and measurement of OAM components. Inset (a) shows the calculated computer holograms for generating the beams carrying fractional OAM. Inset (b) shows the helical phase profiles loaded on the second SLM.

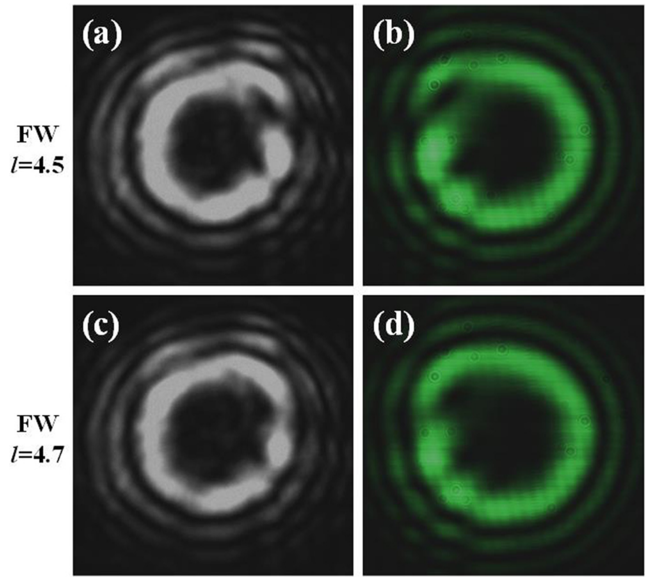

FIG. 2. The intensity profiles of the FWs with $M = 4.5$ (a) and $M = 4.7$ (c); the corresponding intensity profiles of the generated SHs for FW with $M = 4.5$ (b) and $M = 4.7$ (d).

temperature in a periodically poled $LiNbO_3$ (PPLN) crystal with a poling period of 6.8 μm. Since the modulation efficiency of SLM is dependent on the polarization of the incident light, a half-wave plate is used to rotate the polarization direction after filtering the fundamental infrared wave. The third part is designed to measure the distribution of the OAM components of the SH waves, and the method is described in the following. By reflecting the SH wave at the second phase-only SLM, a spiral phase profile $\exp(-im\varphi)$ would be imprinted on the beam wave-front. According to Ref. 26, on the Fourier plane of the reflected field, the photons carrying OAM of $+m\hbar$ will give a bright spot at the center position of phase singularity, while the other OAM components will still have an annular intensity distribution around the singularity. The focusing length of the Fourier lens is about 50 cm, and the typical diameter of the central bright spot is around 60–70 μm.The intensity of the corresponding OAM component can be measured with a power-meter by putting an aperture aligned to the singularity on the Fourier plane, ensuring only the central bright spot passing through the aperture. The aperture size is chosen to be slightly larger than the central spot and we adjusted the aperture size when measuring different orders of integer OAM components.

In the experiment, the topological charge M of the incident FW was chosen to be 4.5 and 4.7 for comparison. We captured the intensity profiles of both the FWs and the corresponding SH waves, as shown in Figure 2. From Figures 2(a) and 2(c), we can find that the intensity profile of the beam carrying non-integer OAM is not a perfect ring and a dark stripe exists.[27] Meanwhile, the patterns of the SH waves shown in Figures 2(b) and 2(d) are not completely circularly distributed when the topological charge of the FW is a non-integer. The results indicate that the SH wave generated in the experiment might have more than one OAM component.

Figure 3 gives the theoretical and experimental OAM distributions of the FW and SH waves, respectively, for both cases with different input fundamental states. The experimental data were measured based on the third part described in the experimental setup. The theoretical OAM spectra of the fundamental waves, shown in Figures 3(a) and 3(b), were calculated according to $P_m(M) = \frac{\sin^2(\mu\pi)}{(M-m)^2\pi^2}$.[22] In the formula, $P_m(M)$ is the probability of any integer state m for a fractional state M, and $\mu \in [0, 1)$ is the fractional part of M. From the figure, we find that the components at $m = 4$ and $m = 5$ have the maximum probability for $M = 4.5$, while for $M = 4.7$, most of the energy is concentrated on $m = 5$. The theoretical OAM distributions of the SH waves were obtained by numerically solving the coupled wave equations in the above. During the calculation, only four dominant integer components of the input fractional OAM state were taken into consideration. It is reasonable for this approximation, because the probabilities are peaked around the nearest integer to M. The polarizations of the 1064-nm FW and the 532-nm SH were both along the c-axis of the $LiNbO_3$ crystal; thus, the nonlinear coefficient used in the simulations is chosen to be about $d_{\mathrm{eff}} = 34.3\,\mathrm{pm/V}$.[28] The values of all the spatial overlapping integrals used in simulations are listed in Table I.

From Figure 3(c) we can see, for the FW carrying topological charge $M = 4.5$, the SH wave has a major OAM component at $l = 9$ which resulting from the sum of the two dominant OAM component 4 and 5 of the FW. While for the two side peaks locating at $l = 8$ and $l = 10$, they come from a doubling of the two dominant components of the FW, respectively. At a fixed nonlinear coefficient, the nonlinear conversion efficiency is proportional to the intensities of the interacting waves as well as the spatial overlapping integrals. There are two equivalents of OAM component of 4 and 5 for the FW, so theoretically the probabilities of the OAM

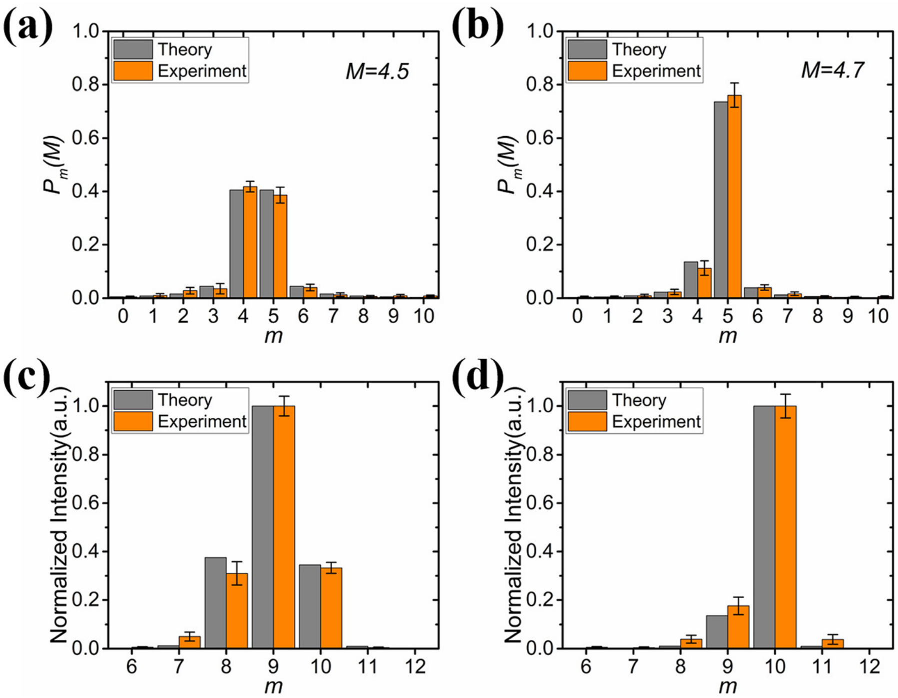

FIG. 3. Theoretical and experimental OAM spectra of the FW with $M = 4.5$ (a) and $M = 4.7$; theoretical and experimental OAM spectra of the generated SH waves when the FW carrying OAM at $M = 4.5$ (c) and 4.7 (d).

components of the generated SH wave at 8 should be greater than that at 10, taking into account the spatial overlapping integrals of the two processes (Table I). However, in Figure 3(c), the measured probabilities at 8 was smaller than those at 10, and this deviation mainly raises from the following two aspects: first, the transmission efficiency of the aperture will change for different aperture sizes, thus leading to different detection efficiencies for different OAM components; second, there would be phase calibration error of the SLM. Besides, only four integer OAM components of the input fractional state are taken into account during numerical calculations, which will cause some small deviations between the theoretical and experimental results in Figs. 3(c) and 3(d), respectively. What one should note is that the coefficient in the coupled wave equations is $\frac{\omega_3 d_{\text{eff}}}{n_3 c}$ for a degenerate second-order nonlinear process, while this coefficient should be doubled for a non-degenerate process,[23] and this is the main reason which leads to a large unequal probability between the components 8 (or 10) and 9 of the SH. Following the similar trend, Figure 3(d) shows that the output SH field has a major component at $l = 10$ when $M = 4.7$, while the amplitudes of the other components are small. This is because the dominant integer OAM component of the FW is located at $m = 5$, which has a probability about 5 times larger than the component at $m = 4$.

The results confirm that the fractional OAM state cannot be regarded as an eigenstate of free space vortex beams. If the fractional state is the eigenstate of vortex beam, the SH wave will have a pure integer state for an input FW carrying half-integer OAM state (e.g., $M = 4.5$). But our experimental results show that, in addition to the OAM component at the doubled state $2M$, there are some other integer OAM components which come from the interaction of the infinite components of the input. In contrast, for the FW carrying non-half-integer (e.g., $M = 4.7$) OAM, if the topological charge of the generated SH wave is $L = 9.4$, its projection on $l = 9$ should have the highest probability according to the equation in Ref. 22. However, both theoretical and experimental results in Figure 3(d) show a different situation—the highest probability occurs at the component $l = 10$ instead of at $l = 9$.

To conclude, we have studied the topological charge transfer during SHG of the incident photons carrying fractional OAM. Owing to the fact that a fractional OAM state can be regarded as the superposition of infinite integer OAM states, we proposed a set of coupled wave equations to describe the frequency doubling process of the fractional OAM state, where the mutual interaction of the integer OAM states were considered. In the experiment, the SHG was realized in a PPLN crystal, and the OAM components of the generated SH waves were measured. For the input FW with a half-integer topological charge $M = 4.5$, the dominant component of the SH located at $l = 9$, which resulted from the summing of the two major components m = 4 and 5 of the FW. While the major component of the SH was located at $l = 10$, which came from the doubling of the major component $m = 5$ of the non-half-integer input $M = 4.7$. The experimental results were in good agreement with the theoretical predictions obtained by numerically solving the coupled

TABLE I. Values of spatial overlapping integrals used in the numerical simulation for different topological charge transfer processes.

Process	$\gamma^{(1,2)}$	$\gamma^{(j,3)}$
$3 + 3 \rightarrow 6$	0.5682	0.5701
$3 + 4 \rightarrow 7$	0.5559	0.5587
$3 + 5 \rightarrow 8$	0.5465	0.5505
$3 + 6 \rightarrow 9$	0.5338	0.5391
$4 + 4 \rightarrow 8$	0.5406	0.5440
$4 + 5 \rightarrow 9$	0.5296	0.5342
$4 + 6 \rightarrow 10$	0.5147	0.5203
$5 + 5 \rightarrow 10$	0.5191	0.5241
$5 + 6 \rightarrow 11$	0.5043	0.5102
$6 + 6 \rightarrow 12$	0.4895	0.4964

wave equations. Our results may lead to better understanding of nonlinear frequency up-conversions of the fractional OAM state.

See supplementary material for a detailed derivation of the coupled wave equations describing second harmonic generation of the fractional OAM state.

This work was supported by the National Natural Science Foundation of China (11674171, 11274165, and 91321312), the National Basic Research Program of China (2012CB921804), the Jiangsu Science Foundation (BK20151374), and PAPD of Jiangsu Higher Education Institutions.

[1] L. Allen, M. W. Beijersbergen, R. J. C. Spreeuw, and J. P. Woerdman, Phys. Rev. A **45**, 8185 (1992).
[2] D. G. Grier, Nature **424**, 810 (2003).
[3] M. P. MacDonald, L. Paterson, K. Volke-Sepulveda, J. Arlt, W. Sibbett, and K. Dholakia, Science **296**, 1101 (2002).
[4] S. Bernet, A. Jesacher, S. Furhapter, C. Maurer, and M. Ritsch-Marte, Opt. Express **14**, 3792 (2006).
[5] A. Mair, A. Vaziri, G. Weihs, and A. Zeilinger, Nature **412**, 313 (2001).
[6] D. S. Ding, Z. Y. Zhou, B. S. Shi, and G. C. Guo, Nat. Commun. **4**, 2527 (2013).
[7] M. W. Beijersbergen, R. P. C. Coerwinkel, M. Kristensen, and J. P. Woerdman, Opt. Commun. **112**, 321 (1994).
[8] L. Marrucci, C. Manzo, and D. Paparo, Phys. Rev. Lett. **96**, 163905 (2006).
[9] P. Chen, W. Ji, B. Wei, W. Hu, V. Chigrinov, and Y. Q. Lu, Appl. Phys. Lett. **107**, 241102 (2015).
[10] N. R. Heckenberg, R. McDuff, C. P. Smith, and A. G. White, Opt. Lett. **17**, 221 (1992).
[11] D. Naidoo, F. S. Roux, A. Dudley, I. Litvin, B. Piccirillo, L. Marrucci, and A. Forbes, Nat. Photonics **10**, 327 (2016).
[12] X. Cai, J. Wang, M. J. Strain, B. Johnson-Morris, J. Zhu, M. Sorel, J. L. O'Brien, M. G. Thompson, and S. Yu, Science **338**, 363 (2012).
[13] K. Dholakia, N. B. Simpson, M. J. Padgett, and L. Allen, Phys. Rev. A **54**, R3742(R) (1996).
[14] N. V. Bloch, K. Shemer, A. Shapira, R. Shiloh, I. Juwiler, and A. Arie, Phys. Rev. Lett. **108**, 233902 (2012).
[15] X. Fang, G. Yang, D. Wei, D. Wei, R. Ni, W. Ji, Y. Zhang, X. Hu, W. Hu, Y. Q. Lu, S. N. Zhu, and M. Xiao, Opt. Lett. **41**, 1169 (2016).
[16] A. Beržanskis, A. Matijošius, A. Piskarskas, V. Smilgevičius, and A. Stabinis, Opt. Commun. **150**, 372 (1998).
[17] G. Gariepy, J. Leach, K. T. Kim, T. J. Hammond, E. Frumker, R. W. Boyd, and P. B. Corkum, Phys. Rev. Lett. **113**, 153901 (2014).
[18] D. D. Hickstein, F. J. Dollar, P. Grychtol, J. L. Ellis, R. Knut, C. Hernández-García, D. Zusin, C. Gentry, J. M. Shaw, T. Fan, K. M. Dorney, A. Becker, A. Jaroń-Becker, H. C. Kapteyn, M. M. Murnane, and C. G. Durfee, Nat. Photonics **9**, 743 (2015).
[19] J. Arlt, K. Dholakia, L. Allen, and M. J. Padgett, Phys. Rev. A **59**, 3950 (1999).
[20] S. S. R. Oemrawsingh, X. Ma, D. Voigt, A. Aiello, E. R. Eliel, G. W. 't Hooft, and J. P. Woerdman, Phys. Rev. Lett. **95**, 240501 (2005).
[21] S. M. Li, L. J. Kong, Z. C. Ren, Y. Li, C. Tu, and H. T. Wang, Phys. Rev. A **88**, 035801 (2013).
[22] J. B. Gǒtte, S. Franke-Arnold, R. Zambrini, and S. M. Barnett, J. Mod. Opt. **54**, 1723 (2007).
[23] R. W. Boyd, *Nonlinear Optics*, 3rd ed. (Elsevier, 2010).
[24] X. P. Hu, P. Xu, and S. N. Zhu, Photonics Res. **1**, 171 (2013).
[25] M. V. Berry, J. Opt. A: Pure Appl. Opt. **6**, 259 (2004).
[26] J. Řeháček, Z. Bouchal, R. Čelechovský, Z. Hradil, and L. L. Sánchez-Soto, Phys. Rev. A **77**, 032110 (2008).
[27] J. Leach, E. Yao, and M. J. Padgett, New J. Phys. **6**, 71 (2004).
[28] M. M. Choy and R. L. Byer, Phys. Rev. B **14**, 1693 (1976).